**Brief Communication**

# G-quadruplex structure improves the immunostimulatory effects of CpG oligonucleotides

Kazuaki Hoshi,[1] Tomohiko Yamazaki,[2]* Yuuki Sugiyama,[1] Kaori Tsukakoshi,[1] Wakako Tsugawa,[1] Koji Sode,[3] and Kazunori Ikebukuro[1]

[1] Department of Biotechnology and Life Science, Graduate School of Engineering, Tokyo University of Agriculture & Technology, Koganei, Tokyo, Japan

[2] Research Center for Functional Materials, National Institute for Materials Science (NIMS), Tsukuba, Japan

[3] Joint Department of Biomedical Engineering, The University of North Carolina at Chapel Hill and North Carolina State University, Chapel Hill, NC, United States

*Corresponding Author

Correspondence: [Tomohiko Yamazaki.]
Research Center for Functional Materials, National Institute for Materials Science,
1-2-1 Sengen, Tsukuba, Ibaraki 305-0047, JAPAN
Tel [+812 9859 2345]
Fax [+812 9860 4741]
Email YAMAZAKI.Tomohiko@nims.go.jp

Authors:

Kazuaki Hoshi [1] [s161082y@st.go.tuat.ac.jp]

Tomohiko Yamazaki [2]* [YAMAZAKI.Tomohiko@nims.go.jp]

Yuuki Sugiyama [1] [ornatanile23@gmail.com]

Kaori Tsukakoshi [1] [k-tsuka@cc.tuat.ac.jp]

Wakako Tsugawa [1] [tsugawa@cc.tuat.ac.jp]

Koji Sode [3] [ksode@email.unc.edu]

Kazunori Ikebukuro [1] [ikebu@cc.tuat.ac.jp]

[1] Department of Biotechnology and Life Science, Graduate School of Engineering, Tokyo University of Agriculture & Technology, Koganei, Tokyo, Japan

[2] Research Center for Functional Materials, National Institute for Materials Science (NIMS), Tsukuba, Japan

[3] Joint Department of Biomedical Engineering, The University of North Carolina at Chapel Hill and North Carolina State University, Chapel Hill, NC, United States

**ABSTRACT**

Single strand oligodeoxynucleotides containing unmethylated cytosine-phosphate-guanine (CpG ODNs) are recognized by the toll-like receptor 9, a component of the innate immunity. Therefore they could act as immunotherapeutic agents. Chemically modified CpG ODNs containing a phosphorothioate (PS) backbone instead of phosphodiester (PD) were developed as immunotherapeutic agents resistant to nuclease degradation. However they cause adverse side effects, so there is a necessity to generate novel CpG ODNs. In the present study, we designed a nuclease-resistant non-modified CpG ODN that forms G-quadruplex structures. G-quadruplex formation in CpG ODNs increased nuclease resistance and cellular uptake. The CpG ODNs designed in this study induced interleukin-6 production in a human B lymphocyte cell line and human peripheral blood mononuclear cells. These results indicate that G-quadruplex formation can be used to increase the immunostimulatory activity of CpG ODNs having a natural PD backbone.

**Introduction**

The toll-like receptor 9 (TLR9) is a component of the innate immunity expressed by human plasmacytoid dendritic cells (pDCs) and B cells that recognize the unmethylated cytosine-phosphate-guanine (CpG) motif present in microbial and viral DNA [1]. TLR9 activation initiates the NF-kappa B signaling pathway that induces the production of cytokines such as tumor necrosis factor (TNF)-$\alpha$, and interleukins (IL)-6 and -12. This pathway also leads to dendritic cell (DC) activation and maturation [2,3]. Single-stranded oligodeoxynucleotides containing the CpG motif (CpG ODNs) mimic the action of microbial DNA. Therefore, they have attracted much attention as vaccine adjuvants and immunotherapy agents for cancers and allergies [4-6]. However, CpG ODNs are very sensitive to degradation by nucleases present in biological fluids such as serum, which limits their immunoregulatory effects.

An alternative for increasing the stability of CpG ODNs against nucleases is to partially or entirely replace the phosphodiester (PD) bonds that link the nucleotides together by phosphorothioate (PS) bonds. Class-A (type D) ODNs consist of palindromic CpG motifs connected by PD bonds in the center of the structure and poly-G tails attached by PS bonds at the 5' and 3' ends. This class of ODNs activates pDCs leading to increased production of IFN-$\alpha$ [7]. Class-B (type K) ODNs consist exclusively of PS bonds and stimulate the proliferation and activation of B cells [8]. Class-C ODNs include one or two CpG motifs with PD linkage and palindromic sequences with PS linkage at the 3' end; they activate both pDCs and B cells [9]. Class-P ODNs include two palindromic CpG motifs containing PS bonds exclusively and lead to the

production of higher amounts of type-I interferon than Class-C ODNs [10]. However, there is a concern about the safety of these molecules because adverse side effects associated with the PS backbone have been reported [11]. Consequently, the synthesis of nuclease-resistant CpG ODNs containing a PD backbone is attractive for the development of safer immunotherapies.

One way to increase DNA stability without making backbone modifications is to induce the formation of G-quadruplex (G4) structures. The G4 is a noncanonical secondary structure of DNA containing stacked G-quartet planes of four guanines connected by a network of Hoogsteen hydrogen bonds [12]. Regions of G-rich repeats capable of forming G4 are abundant in telomeric DNA, at the end of the chromosomes, and may play an essential role in preventing inappropriate elongation by telomerase, nucleolytic degradation, and end-to-end fusions [12]. G4 structures are topologically polymorphic and are classified based on the participation of one (intramolecular) or many (intermolecular) DNA strands; and on the DNA strand orientation, G4 configurations are mainly divided into parallel, anti-parallel, and hybrid [13], the arrangements are determined by measuring the circular dichroism (CD) spectra of the DNA. Bishop et al. developed a nuclease-resistant form of anti-HIV ODNs, exclusively with PD bonds, containing a G4 motif [14]. These results indicate that inducing G4 formation may be useful for developing nuclease-resistant immunostimulatory CpG ODNs with a complete PD linkage.

In the present study, we aimed to test this hypothesis. To do so, we designed ODNs containing both CpG motifs and poly-G regions to induce G4 formation. We evaluated the stability of the G4-CpG ODNs in the

5

serum, and their ability to induce cellular uptake and cytokine production by a human B lymphocyte cell line

and human peripheral blood mononuclear cells (PBMCs).

**Materials and Methods**

**Preparation of G4- CpG ODNs**

The CpG ODNs used in this study were synthesized by Eurofins Genomics (Tokyo, Japan) and purified by high-performance liquid chromatography (HPLC), the sequences are shown in Table 1. The ODNs were dissolved in sterile deionized water to a concentration of 100 μM for further analysis. To induce G4 structure formation, the CpG ODNs were diluted in Dulbecco's phosphate-buffered saline without calcium and magnesium (D-PBS(-), 2.68 mM KCl, 137 mM NaCl, 1.47 mM $KH_2PO_4$, and 8.10 mM $Na_2HPO_4$; DS Pharma Biomedical, Osaka, Japan) to a final concentration of 10 μM. The CpG ODNs solution was incubated at 95 °C for 5 min, and then gradually cooled to 30 °C using a TP650 thermal cycler (Takara Bio, Shiga, Japan).

The G4 formation was confirmed by polyacrylamide gel electrophoresis (PAGE). Briefly, CpG ODNs (0.1 μg) were applied to a 15 % PAGE in Tris-glycine buffer (25 mM Tris, 192 mM glycine; ATTO, Tokyo, Japan) and separated by applying 20 mA at 4 °C for 80 min. The CpG ODNs were visualized by SYBR Gold nucleic acid gel stain (Thermo Fisher Scientific, Waltham, MA, US) fluorescence.

**Measurement of Circular Dichroism (CD) Spectroscopy**

CpG ODNs (20 μM) were folded in a buffer containing 10 mM Tris-HCl pH 8.0, 150 mM KCl, and 10 mM NaCl, as described above. Circular dichroism (CD) spectra were measured using a J-725 spectropolarimeter (JASCO, Tokyo, Japan) and a quartz cell of 10 mm optical path length (JASCO) at 25 °C.

Scanning was performed from 220 nm to 320 nm at 25 °C with a resolution of 0.2 nm, a bandwidth of 10 nm, and scan speed of 50 nm/min. Each scan was repeated 10 times, and the values were averaged. The buffer sample spectrum was subtracted to eliminate background. For CD melting and annealing experiments, CD measurement was performed at 267 nm with a heating or cooling rate of 1.0 °C min$^{-1}$.

**Measurement of the thermal difference spectrum**

$G_4$-CpG (10 µM) was folded in D-PBS(-) as described above. The absorbance spectra of $G_4$-CpG at 20 °C and 90 °C were measured using a spectrophotometer V-670 (JASCO, Tokyo, Japan). The thermal difference spectrum (TDS) was obtained by subtracting the absorbance spectrum at 20 °C from that at 90 °C. The absorbance at 295 nm was monitored with a heating or cooling rate of 0.2 °C min$^{-1}$ to examine the melting and annealing curves of $G_4$-CpG.

**Stability Assay in Serum**

To evaluate the stability of CpG ODNs against nucleases present in the serum, 4 µl of 10 µM folded CpG ODNs were added to 36 µL of 20% (v/v) fetal bovine serum (FBS; Thermo Fisher Scientific; The final concentration of FBS in the test was 18 % (v/v)) and incubated at 37 °C for 0, 1, 2, 4, and 24 hours. The reaction was terminated by adding 4 µl of 250 mM EDTA solution and heating at 80 °C for 2 min. The samples were stored at 4 °C until analyzed by PAGE. The fluorescence intensity of each band was quantified

using the Image Studio™ Lite software (LI-COR Biotechnology, Lincoln, NE, US).

**Cellular Culture**

The human B lymphocyte cell line, Namalwa cells (IFO50040; Japanese Collection of Research Bioresources Cell Bank) was cultured in RPMI1640 (#11875-093; Thermo Fisher Scientific) supplemented with 10% (v/v) FBS, 10 mM HEPES, 50 U/ml penicillin, and 50 µg/ml streptomycin at 37 °C in a humidified incubator containing 5% $CO_2$.

**Cellular Uptake Assay**

The culture medium of Namalwa cells was replaced with Opti-MEM medium (Thermo Fisher Scientific) at a density of $5.0 \times 10^5$ cells/ml. Then, 200 µl of cell suspension was seeded in a 96-well plate. CpG ODNs labeled with 6-carboxyfluorescein (6-FAM) at the 3'-end were added to the medium to a final concentration of 5.0 µM. The cells were incubated at 37 °C in a humidified incubator containing 5% $CO_2$ for 2 hours. The cells were washed twice with 500 µl phosphate-buffered saline (PBS) and harvested. The cellular fluorescence intensity was analyzed with a flow cytometer (SP6800; Sony, Tokyo, Japan).

**Measurement of IL-6 Production in Human B Cell Line and PBMC by ELISA**

Namalwa cells were seeded in a 96-well plate at a density of $1.0 \times 10^5$ cells/well and stimulated with

0.5 μM CpG ODNs for 48 hours at 37 °C in a humidified incubator containing 5% $CO_2$.

Commercially available frozen human PBMCs were purchased from Cellular Technology Limited (Shaker Heights, OH, USA). PBMCs were thawed according to the manufacturer's instructions and suspended in RPMI 1640 medium supplemented with 10% (v/v) FBS, 10 mM HEPES, 50 U/ml penicillin, and 50 μg/ml streptomycin, and then seeded in a 96-well plate at a density of $1.0 \times 10^5$ cells/well. PBMCs were stimulated with 0.5 μM CpG ODNs for 24 hours at 37 °C in a humidified incubator containing 5% $CO_2$.

The supernatant was collected and stored at -30 °C until used. The levels of IL-6 secreted into the medium were determined using the Ready-Set-Go! ELISA kit (Thermo Fisher Scientific) according to the manufacturer's instructions.

**Statistical Analysis**

Data are expressed as the mean $\pm$ standard deviation (SD) of five measurements. Statistical differences were evaluated by one-way analysis of variance (ANOVA) followed by the Dunnett's test for multiple comparisons. A p-value below 0.05 was considered to be statistically significant.

**Results and Discussion**

We first designed ODNs capable of forming G4. The sequence GTCGTT linked by a PD backbone is known as the CpG motif recognized by human cells [15]. Meng et al. developed a nuclease-resistant CpG ODNs linked exclusively by PD bonds, containing six GTCGTT repeats (PD-ODN2006-2006) [16]. PD-ODN2006-2006 induces significant levels of TLR9-mediated NF-kappa B activation in PBMCs, leading to high IL-6 production [16]. Based on these results, we designed ODNs containing GTCGTT as the basic sequence. The sequence motif $G_{\geq 3}N_xG_{\geq 3}N_xG_{\geq 3}N_xG_{\geq 3}$ has been reported to form G4 [17]. So, we designed ODNs containing poly-guanine sequences alternating with the CpG motifs (Table 1). $G_0$-CpG did not contain any guanosine between the CpG motifs and was intended to be a linear control. $G_2$-, $G_4$-, and $G_8$-CpG included 2, 4, and 8 guanosine repeats between the CpG motifs, respectively. Since TLR9 activation is abolished by the rearrangement of the cytosine-guanosine (CG) sequence to guanosine-cytosine (GC) in ODNs [2], we designed $G_4$-GpC as a negative control of $G_4$-CpG.

We next examined whether the designed CpG ODNs formed secondary structures by measuring their CD spectra (Fig. 1A). G4 structure formation is driven by monovalent cations such as $Na^+$ and $K^+$ [17]. To induce folding, each ODN was heated and gradually cooled in a buffer containing 150 mM KCl, that mimics the intracellular potassium concentration. The CD spectra of $G_0$-CpG showed a negative peak around 250 nm and a positive peak around 280 nm, this spectrum is characteristic of random coil DNA. $G_2$-CpG presented peaks similar to those of $G_0$-CpG, so we inferred that it did not form the G4 structure.

11

In contrast, $G_4$-CpG and $G_8$-CpG showed a negative peak at 240 nm, and a positive peak at 260 nm. These results correspond to the characteristic spectrum of parallel G4s [18]. Therefore, we concluded that $G_4$- and $G_8$-CpG formed G4 structures in the presence of monovalent cations. To estimate the high-order structures of G4 formed by the CpG ODNs, they were analyzed by PAGE (Fig. 1B). All ODNs showed single bands without any smearing; this suggests that they formed individual structures. $G_0$-CpG (48 mer), showed a migration pattern similar to that of the 50 bp band of the DNA marker (Lane 1). In contrast, $G_2$-CpG (56 mer), and $G_4$-CpG (64 mer) showed a migration pattern similar to that of the 70 bp and 110 bp bands of the DNA marker, respectively (Lane 2-3). From the results of the CD spectra, we expected $G_4$-CpG to form unimolecular G4. However, the PAGE results did not support our hypothesis. We then measured the absorbance spectra of the unfolded and folded states of $G_4$-CpG to obtain the TDS and evaluate G4 formation. The denaturation of the G4 structure is characterized by a negative peak around 295 nm in the TDS [19]. The spectrum of $G_4$-CpG had a negative peak around at 295 nm, indicating that the G4 structure was denaturated (Fig.1C). The result of TDS indicated that $G_4$-CpG formed the G4 structure. To confirm the stated molecularity of G4-CpG, we also performed the CD melting and annealing experiments by monitoring at 267 nm (Supplementary Fig.1). $G_4$-CpG shows reversible melting with considerable difference between melting and annealing, where melting and annealing curves were not superimposable. After the annealing, we heated the ODNs again and the 2nd melting curves were superimposable with 1st melting curves (Supplementary Fig.1A). The melting and annealing curves of $G_4$-CpG were also examined by monitoring

12

at the absorbance at 295 nm. The melting/annealing curves were not superimposable as well as seen in the CD melting/annealing experiments (Supplementary Fig.1B). From these results, $G_4$-CpG might form the various G4 structures and lead the formation of the G4 multimer.

In contrast, $G_8$-CpG ODNs did not enter the gel (Lane 4, Fig.1B). The GGGGTTGGGG sequence forms intermolecular G4 which leads to oligomer formation, called G-wires [20]. Klein et al. proposed that Class-A ODNs form intermolecular G4 which leads to multimer formation [21]. Thus, it is possible that $G_8$-CpG forms G-wire structures that are too big to enter the gel. CpG ODNs that form uncontrollable high order structures cannot be used for clinical applications. Contrarily, $G_4$-CpG formed controllable G4 structure and did not lead to G-wire formation.

We incubated $G_4$-CpG and $G_0$-CpG in FBS to investigate their stability against serum nucleases. At different incubations times, the ODNs were separated by PAGE to evaluate degradation (Fig. 1D). $G_0$-CpG was almost completely degraded after 1-hour incubation, indicating a low resistance to nuclease action. In contrast, the band corresponding to $G_4$-CpG was apparent after 4 hours incubation, and after 24 hours the band had no completely disappeared. This suggests that by inserting GGGG between the CpG motifs, the CpG ODNs with PD linkage folded into G4s and became more resistant to nucleases. Our results agree with previous reports by Li et al. that showed that CpG bearing DNA tetrahedral nanostructures are not degraded after 4 hours of incubation in serum and that they can induce TNF-$\alpha$, IL-6, and IL-12 release [22]. It has been reported that the formation of secondary structures such as Y-shaped and dendrimer-like (DL) DNA

containing CpG motifs increases their cellular uptake [23,24]. So, we examined whether G4 structures in

CpG ODNs increased their cellular uptake by the human B lymphocyte cell line, Namalwa cells. 6-FAM-

labeled $G_0$-CpG and $G_4$-CpG were added to the culture medium of Namalwa cells for 2 hours, and the cellular

fluorescence intensity was measured by flow cytometry (Fig. 1E). When the cells were incubated with $G_4$-

CpG, the mean fluorescence intensity (MFI) was more than 10-fold that of cells incubated with $G_0$-CpG. Just

as Y and DL-DNAs, G4 formation in CpG ODNs increased the cellular uptake by the immune cells. Opazo

et al. demonstrated that the mutation of guanines, which form the G-tetrad of G4, decreases the cellular

uptake into Burkitt's lymphoma cells [25]. The G4 structure may affect the efficiency of cellular uptake and

be useful for developing CpG ODNs with increase cellular uptake.

Moreover, Zhang et al. showed that the morphological features of nanodiamonds affect both the

anchoring and internalization stages of endocytosis [26]. A round nanodiamond is more effectively

internalized by the cells than a prickly nanodiamond even though both surfaces are composed by similar

functional groups [26]. Thus, the shape of ODNs may also affect cellular uptake efficiency.

As TLR9 localizes in the endosomal compartment of mammalian cells, CpG ODNs need to be

incorporated into the cells and transported to the endosomes to activate it. Since $G_4$-CpG showed increased

nuclease resistance and cellular uptake, we expected that it would localize to the endosomal compartment

and activate TLR9, resulting in a more efficient induction of inflammatory cytokine production by B cells

than that of CpG ODNs with random structure. To measure this, we incubated Namalwa cells with all the

ODNs designed in this study and measured IL-6 production. Fig. 2A shows the IL-6 measurement by ELISA. After 48 hours of incubation, $G_4$-CpG induced IL-6 production more than 7-fold that of $G_0$-CpG. G-wire-forming $G_8$-CpG did not significantly stimulate Namalwa cells. Furthermore, the level of IL-6 induced by $G_4$-GpC was significantly lower than that of $G_4$-CpG, indicating that the G4 structure itself did not activate TLR9. These results suggest that the immunostimulatory effect of the CpG motif can be significantly enhanced by G4 formation.

We also assessed the potential of G4-CpG-ODNs using human PBMCs, which consist of lymphocytes (T cells, B cells, and NK cells), monocytes, and dendritic cells. $G_4$-CpG induced IL-6 production by PBMCs, while $G_0$-$C_P$G did not (Fig. 2B). We can conclude that the increased stability and cellular uptake induced by G4 formation resulted in increased IL-6 production by primary immune cells.

In the present study, we demonstrated that G4 formation might be useful for the development of immunostimulatory CpG ODNs. G4 formation contributes to the transport of CpG ODNs into the endosomal compartment, by enhancing the stability and cellular uptake of the nucleotides, leading to a high IL-6 production in immune cells. G4 structures are topologically very polymorphic depending on their sequences and folding condition. Therefore, the development of G4-CpG-ODNs with higher stability could be achieved by controlling their topology and might be used in the development of human immunotherapeutic agents.

**Acknowledgments**

**Author Disclosure Statement**

No competing financial interests exist.

**References**

1. Hornung V, Rothenfusser S, Britsch S, Krug A, Jahrsdorfer B, Giese T, Endres S and Hartmann G. (2002). Quantitative Expression of Toll-Like Receptor 1-10 mRNA in Cellular Subsets of Human Peripheral Blood Mononuclear Cells and Sensitivity to CpG Oligodeoxynucleotides. J Immunol 168:4531–4537.

2. Bauer S, Kirschning CJ, Hacker H, Redecke V, Hausmann S, Akira S, Wagner H and Lipford GB. (2001). Human TLR9 confers responsiveness to bacterial DNA via species-specific CpG motif recognition. Proc Natl Acad Sci 98:9237–9242.

3. Montoya CJ, Jie H-B, Al-Harthi L, Mulder C, Patiño PJ, Rugeles MT, Krieg AM, Landay AL and Wilson SB. (2006). Activation of plasmacytoid dendritic cells with TLR9 agonists initiates invariant NKT cell-mediated cross-talk with myeloid dendritic cells. J Immunol 177:1028–1039.

4. Cho HJ, Takabayashi K, Cheng PM, Nguyen MD, Corr M, Tuck S and Raz E. (2000). Immunostimulatory DNA-based vaccines reduce cytotoxic lymphocyte activity by a T-helper cell-independent mechanism. Nat Biotechnol 18:509–514.

5. Suzuki M, Ohta N, Min WP, Matsumoto T, Min R, Zhang X, Toida K and Murakami S. (2007). Immunotherapy with CpG DNA conjugated with T-cell epitope peptide of an allergenic Cry j 2 protein is useful for control of allergic conditions in mice. Int Immunopharmacol 7:46–54.

6. Chu RS, Targoni OS, Krieg AM, Lehmann PV and Harding CV. (1997). CpG Oligodeoxynucleotides Act as Adjuvants that Switch on T Helper 1 (Th1) Immunity. J Exp Med 186:1623–1631.

7. Krug A, Rothenfusser S, Hornung V, Jahrsdrfer B, Blackwell S, Ballas ZK, Endres S, Krieg AM and Hartmann G. (2001). Identification of CpG oligonucleotide sequences with high induction of IFN-α/β in plasmacytoid dendritic cells. Eur J Immunol 31:2154–2163.

8. Hartmann G, Weeratna RD, Ballas ZK, Payette P, Blackwell S, Suparto I, Rasmussen WL, Waldschmidt M, Sajuthi D, Purcell RH, Davis HL and Krieg AM. (2000). Delineation of a CpG Phosphorothioate Oligodeoxynucleotide for Activating Primate Immune Responses In Vitro and In Vivo. J Immunol 164:1617–1624.

9. Vollmer J, Weeratna R, Payette P, Jurk M, Schetter C, Laucht M, Wader T, Tluk S, Liu M, Davis HL and Krieg AM. (2004). Characterization of three CpG oligodeoxynucleotide classes with distinct immunostimulatory activities. Eur J Immunol 34:251–262.

10. Samulowitz U, Weber M, Weeratna R, Uhlmann E, Noll B, Krieg AM and Vollmer J. (2010). A Novel Class of Immune-Stimulatory CpG Oligodeoxynucleotides Unifies High Potency in Type I Interferon Induction with Preferred Structural Properties. Oligonucleotides 20:93–101.

11. Brown DA, Kang SH, Gryaznov SM, DeDionisio L, Heidenreich O, Sullivan S, Xu X and Nerenberg MI. (1994). Effect of phosphorothioate modification of oligodeoxynucleotides on specific protein binding. J Biol Chem 269:26801–26805.

12. Rhodes D and Lipps HJ. (2015). Survey and summary G-quadruplexes and their regulatory roles in biology. Nucleic Acids Res 43:8627–8637.

13. Bryan TM and Baumann P. (2011). G-quadruplexes: From guanine gels to chemotherapeutics. Mol Biotechnol 49:198–208.

14. Bishop JS, Guy-Caffey JK, Ojwang JO, Smith SR, Hogan ME, Cossum PA, Rando RF and Chaudhary N. (1996). Intramolecular G-quartet motifs confer nuclease resistance to a potent anti-HIV oligonucleotide. J Biol Chem 271:5698–5703.

15. Hartmann G and Krieg AM. (2000). Mechanism and Function of a Newly Identified CpG DNA Motif in Human Primary B Cells. J Immunol 164:944–953.

16. Meng W, Yamazaki T, Nishida Y and Hanagata N. (2011). Nuclease-resistant immunostimulatory phosphodiester CpG oligodeoxynucleotides as human Toll-like receptor 9 agonists. BMC Biotechnol 11:88.

17. Maizels N and Gray LT. (2013). The G4 Genome. PLoS Genet 9:e1003468.

18. Zhou B, Liu C, Geng Y and Zhu G. (2015). Topology of a G-quadruplex DNA formed by C9orf72 hexanucleotide repeats associated with ALS and FTD. Sci Rep 5:16673.

19. Mergny JL, Phan AT and Lacroix L. (1998). Following G-quartet formation by UV-spectroscopy. FEBS Lett 435:74–78.

20. Marsh TC, Vesenka J and Henderson E. (1995). A new DNA nanostructure, the G-wire, imaged by scanning probe microscopy. Nucleic Acids Res 23:696–700.

21. Klein DCG, Latz E, Espevik T and Stokke BT. (2010). Higher order structure of short immunostimulatory oligonucleotides studied by atomic force microscopy. Ultramicroscopy 110:689–693.

22. Li J, Pei H, Zhu B, Liang L, Wei M, He Y, Chen N, Li D, Huang Q and Fan C. (2011). Self-assembled multivalent DNA nanostructures for noninvasive intracellular delivery of immunostimulatory CpG oligonucleotides. ACS Nano 5:8783–8789.

23. Nishikawa M, Matono M, Rattanakiat S, Matsuoka N and Takakura Y. (2008). Enhanced immunostimulatory activity of oligodeoxynucleotides by Y-shape formation. Immunology 124:247–255.

24. Rattanakiat S, Nishikawa M, Funabashi H, Luo D and Takakura Y. (2009). The assembly of a short linear natural cytosine-phosphate-guanine DNA into dendritic structures and its effect on immunostimulatory activity. Biomaterials 30:5701–5706.

25. Opazo F, Eiden L, Hansen L, Rohrbach F, Wengel J, Kjems J and Mayer G. (2015). Modular assembly of cell-targeting devices based on an uncommon G-quadruplex aptamer. Mol. Ther. Nucleic Acids, 4: e251.

26. Zhang B, Feng X, Yin H, Ge Z, Wang Y, Chu Z, Raabova H, Vavra J, Cigler P, Liu R, Wang Y and Li Q. (2017). Anchored but not internalized: Shape dependent endocytosis of nanodiamond. Sci Rep 7:46462.
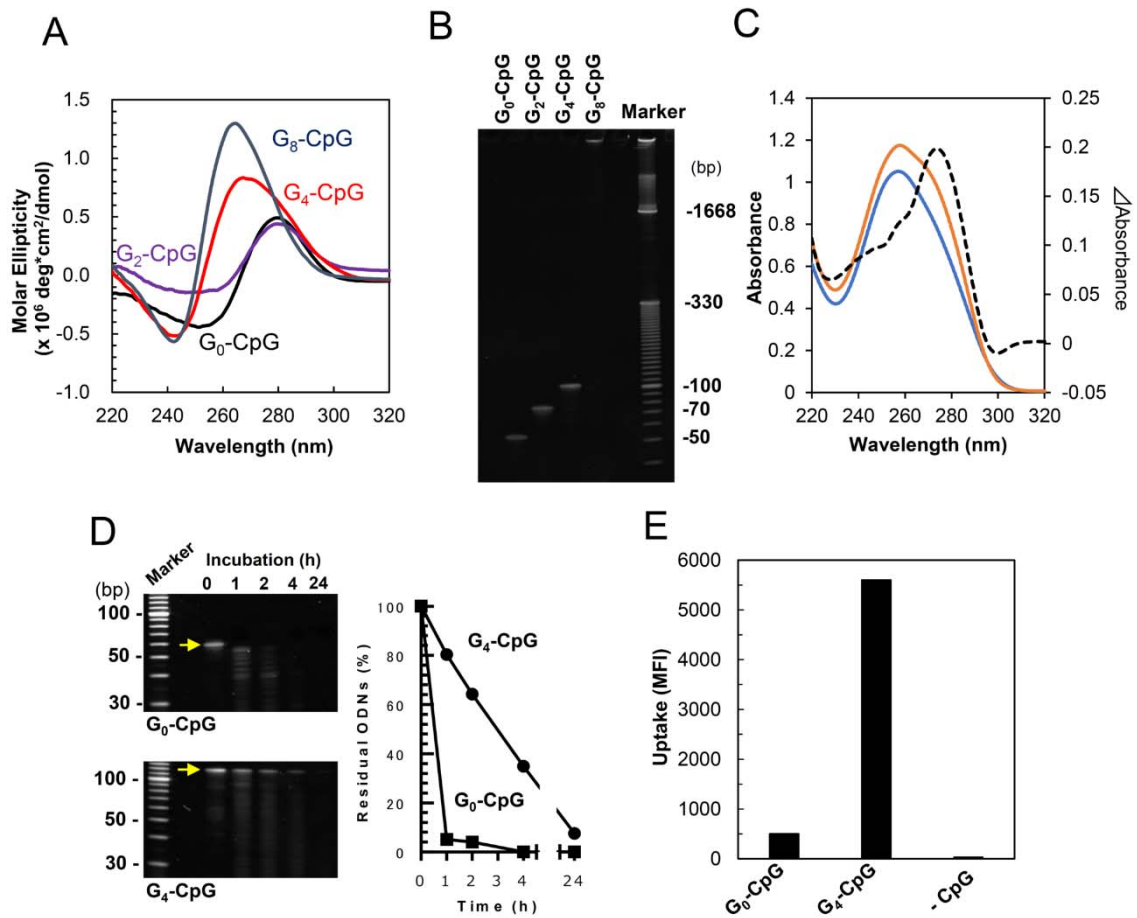
**Tables:**

**Table 1 Sequence of CpG ODNs Used in this Study**

The immunostimulatory CpG motifs (GTCGTT) for human are underlined. Abbreviations: CpG, cytosine-

phosphate-guanine; ODNs, oligodeoxynucleotides.

Please provide the table here.

| Name | Sequence (5'→3') | Length (nucleotides) |
|---|---|---|
| $G_0$-CpG | TTGTCGTTTTGTCGTTTTGTCGTTTTGTCGTTTTGTCGTTTTGTCGTT | 48 |
| $G_2$-CpG | **GG**TTGTCGTTTTGTCGTT**GG**TTGTCGTTTTGTCGTT**GG**TTGTCGTTTTGTCGTT**GG** | 56 |
| $G_4$-CpG | **GGGG**TTGTCGTTTTGTCGTT**GGGG**TTGTCGTTTTGTCGTT**GGGG**TTGTCGTTTTGTCGTT**GGGG** | 64 |
| $G_8$-CpG | **GGGGGGGG**TTGTCGTTTTGTCGTT**GGGGGGGG**TTGTCGTTTTGTCGTT**GGGGGGGG**TTGTCGTTTTGTCGTT**GGGGGGGG** | 80 |
| $G_4$-GpC | **GGGG**TTGTGCTTTTGTGCTT**GGGG**TTGTGCTTTTGTGCTT**GGGG**TTGTGCTTTTGTGCTT**GGGG** | 64 |

19

**Figure 1 Characteristic of G-quadruplex-forming CpG ODNs**
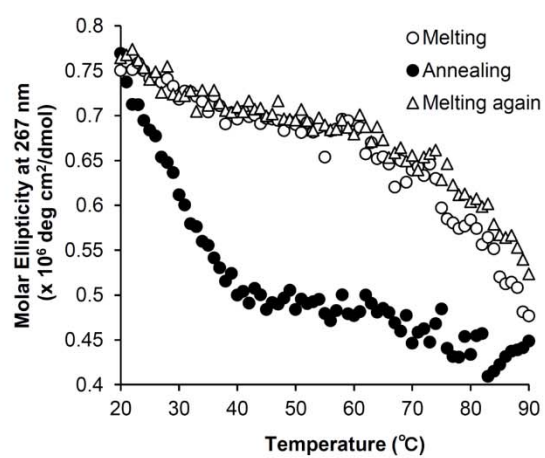
(A) Circular dichroism spectra of G-quadruplex CpG ODNs. Black line, $G_0$-CpG; Purple line, $G_2$-CpG; Red line, $G_4$-CpG; Blue line, $G_8$-CpG. (B) Polyacrylamide gel electrophoresis of G-quadruplex CpG ODNs. Marker, 10 bp DNA Ladder (Thermo Fisher Scientific). (C) TDS analysis of $G_4$-CpG. The TDS (dotted line) results from the subtraction of the 20 °C spectrum (blue line) from the 90 °C spectrum (orange line) (D) Serum stability of $G_0$-CpG and $G_4$-CpG in 18% (v/v) serum containing buffer. Left: Presence of $G_0$-CpG and $G_4$-CpG assessed by polyacrylamide gel electrophoresis. Right: quantification of the bands in the gel corresponding to $G_0$-CpG and $G_4$-CpG. (E) Uptake of fluorescent ODNs by Namalwa cells. Abbreviation: MFI, mean of fluorescence intensity.
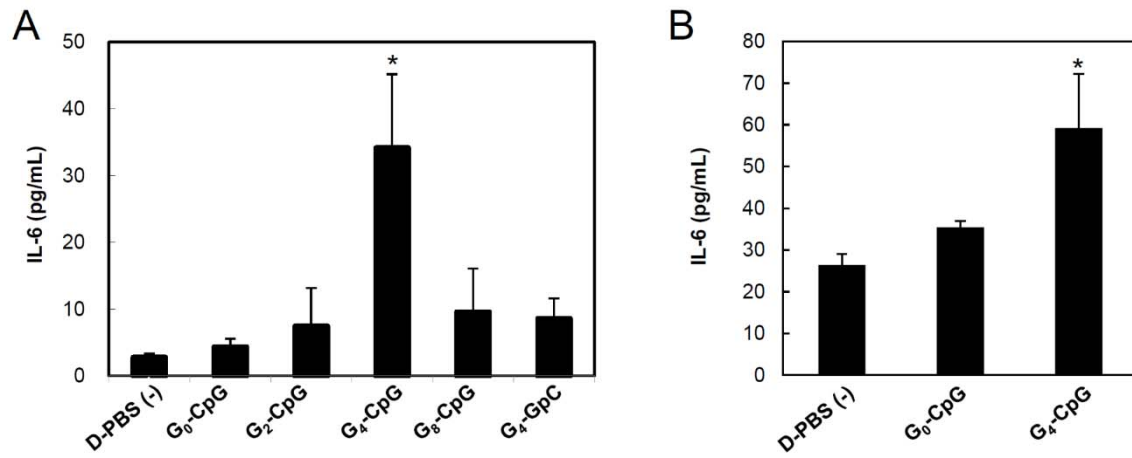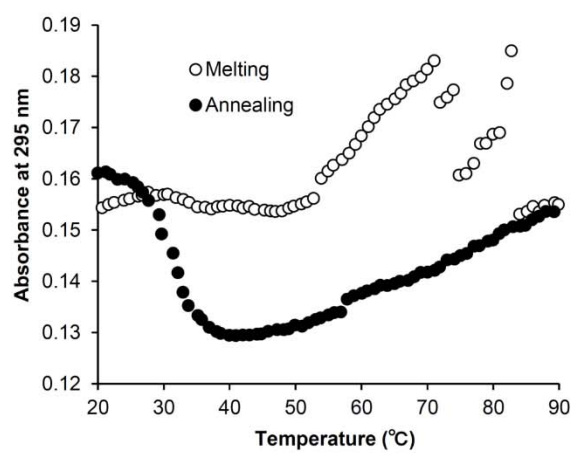
**Figure 2 Levels of IL-6 production induced by CpG ODNs**

(A) Namalwa cells (B) human PBMCs. IL-6 in the supernatant was determined by ELISA. The results are expressed as the mean ± SD of five determinations. *: $p < 0.05$, representing a significant difference from the IL-6 level induced by D-PBS (-).

**Supplementary Fig.1**